

RESEARCH ARTICLE

Hongguang Ma · Judith P. Grassle · Robert J. Chant

Vertical distribution of bivalve larvae along a cross-shelf transect during summer upwelling and downwellingReceived: 5 July 2005 / Accepted: 7 February 2006 / Published online: 29 March 2006
© Springer-Verlag 2006

Abstract Previous time-series studies of meroplankton abundances in the LEO-15 research area off Tuckerton, New Jersey, USA (39°28'N, 74°15'W) indicated short-lived (6–12 h) pulses in larval surfclam (*Spisula solidissima* Dillwyn) concentration often associated with the initiation of downwelling. To examine possible larval surfclam (and other bivalve) concentrating mechanisms during upwelling and downwelling, six sets of adaptive mobile zooplankton pump samples were taken in July 1998 at different depths at five to six stations along a 25-km transect perpendicular to the coastline and crossing Beach Haven Ridge at LEO-15. Sampling was guided by near real-time, satellite imagery of sea surface temperature overlain by sea surface currents from a shore-based ocean surface current radar (OSCR) unit. A Seabird CTD on the mobile pump frame near the intake provided information on thermocline depth, and sampling depths were adjusted according to the temperature profiles. Near shore, the thermocline was tilted down during downwelling, and up during upwelling. The highest concentrations of surfclam larvae occurred near the bottom at a station near Beach Haven Ridge during downwelling, and just above the thermocline 3 km further offshore during well-developed upwelling. For other bivalve taxa, the larvae were concentrated near the thermocline (*Anomia simplex* Orbigny and Pholadidae spp.) or concentrated upslope near the bottom (Mytilidae spp.) during upwelling, and the larvae were concentrated near the bottom or were moved downslope during downwelling. *Donax fossor* Say larvae were found near the surface or above the thermocline during upwelling and downwelling. The general patterns of

larval bivalve distribution appear to be influenced by water mass movement during upwelling and downwelling. The larval concentration patterns of individual species are likely a consequence of advection due to upwelling and downwelling circulation, vertical shear in the front region, species-specific larval behaviors, and larval sources.

Introduction

Studies of benthic macrofaunal communities and the abundance and distribution of the planktonic larvae of selected benthic species with respect to recurrent upwelling and downwelling events in inshore environments on Beach Haven Ridge off Tuckerton, New Jersey, USA (39°28'N, 74°15'W) suggest that physical mechanisms are responsible for creating dense patches of larvae, and that settlement occurs when these concentrations are brought to the bottom during downwelling (Snelgrove et al. 1999, 2001; Weissberger and Grassle 2003; Ma and Grassle 2004; Ma 2005; Ma et al. 2006). In the present study, we sought to identify how wind-driven cross-shelf circulation and the behavior of the larvae of individual bivalve species might interact to produce patches of high larval abundance.

Interest in this topic has quickened since Roughgarden et al. (1991) suggested that barnacle larvae may accumulate in offshore fronts off the coast of California during upwelling. When winds relax and upwelling ceases, the front moves inshore and collides with the coast depositing the larvae accumulated there. Numerous additional studies directed at understanding the relationship between wind-driven cross-shelf and alongshore circulation, and larval transport and settlement have followed on the west coast of the USA (e.g., Farrell et al. 1991; Wing et al. 1995a, b, 1998; Miller and Emler 1997; Connolly and Roughgarden 1999; Shanks and McCulloch 2003; Shanks et al. 2003b) and off Duck, North Carolina, USA (e.g., Shanks et al. 2000, 2002, 2003a; Garland and Zimmer 2002; Garland et al. 2002).

Communicated by R.J. Thompson, St. John's

H. Ma (✉) · J. P. Grassle · R. J. Chant
Institute of Marine and Coastal Sciences,
Rutgers University, 71 Dudley Road,
New Brunswick, NJ 08901, USA
E-mail: hgma@imcs.rutgers.edu
Tel.: +1-732-9326555
Fax: +1-732-9328578

In a 3-year study (1996–1998), we examined near-bottom concentrations of meroplankton every 4 h during upwelling and downwelling conditions off the coast of New Jersey, USA in July (Ma and Grassle 2004). Short-lived pulses of highest concentrations of bivalve larvae (largely composed of surfclam larvae, *Spisula solidissima*) and total gastropod larvae often coincided with the initial downwelling of warm water over two inshore bottom stations on either side of Beach Haven Ridge, a 12- to 15-m deep, shore-oblique sand ridge (the LEO-15 research area). In 1997, a similar coincidence of high larval concentrations and the first appearance of warm water at an offshore bottom station (at 20-m depth) following strong downwelling-favorable winds was also observed.

During the present study, extensive physical observations and modeling studies of upwelling and downwelling (Glenn et al. 1996; Münchow and Chant 2000; Song et al. 2001; Chant et al. 2004; Kohut et al. 2004) have added to our understanding of the physical processes that might be responsible for concentrating larvae in the vicinity of our study site. In May to August each year, sustained southwesterly winds (associated with the subtropical Bermuda High) along the New Jersey coast cause offshore movement of warm surface water and inshore and upward movement of cold bottom water (i.e., coastal upwelling). These upwellings last for days to weeks. When the southwest winds are sustained, an ~50-km long wavelike pattern develops along the upwelling front, and the band of upwelled water forms several isolated cold surface patches or upwelling centers along the New Jersey coast (Glenn et al. 1996; Song et al. 2001), with the LEO-15 research area on Beach Haven Ridge lying within one of these centers. Earlier two-dimensional models of coastal upwelling have been replaced by three-dimensional models which include a divergence/convergence in alongshore currents (Smith 1981) and an alongshore variability caused by a combination of the internal dynamics and the underlying bathymetry. Chant et al. (2004) followed the evolution of an alongshore flow reversal during an upwelling from 20 to 25 July 1998 during our study period. The flow reversal occurred near shore in the form of a subsurface jet with maximum velocities $> 30 \text{ cm s}^{-1}$ which was most intense in the thermocline. The jet veers offshore into the upwelling center due to greater friction over the shoaling and rougher topography toward the south. The flow reversal observed by Chant et al. (2004) was not associated with a buoyant coastal current and so differs from those described by Yankovsky et al. (2000) in the same area. The latter are also of interest with respect to occurrences of high concentrations of certain species of bivalve larvae in the LEO-15 research area, which appear to be associated with the arrival of relatively low salinity water masses during upwelling relaxation and downwelling (Ma and Grassle 2004).

Numerous field distribution studies of bivalve larvae have indicated that, despite their relatively weak swimming abilities with respect to ocean currents and

turbulence, they can, under certain circumstances, affect their horizontal transport by modifying their vertical swimming and sinking behaviors (e.g., Tremblay and Sinclair 1990; Tremblay et al. 1994; Shanks et al. 2000; Garland et al. 2002). These patterns are often very clear with respect to the sharp discontinuities that occur in estuarine water columns (e.g., Gregg 2002; Baker 2003; Baker and Mann 2003). Experimental laboratory studies (e.g., Mann et al. 1991; Gallager et al. 1996; Manuel et al. 1996, 2000; Pearce et al. 1996, 1998) have confirmed that certain larvae will pass through a pycnocline while others do not, and that there is an ontogenetic component to vertical swimming behavior in bivalve larvae so that older larvae approaching metamorphosis may reduce their effective upward swimming component (e.g., Grassle et al. 1992; Gallager et al. 1996). Franks (1992) provides a useful conceptual model of the interactions between larval swimming behaviors and physical processes at convergent and divergent fronts, which generally predicts that organisms are likely to be concentrated in a thin horizontal band crossing isopycnals in a divergent flow, and concentrated along a pycnocline in convergent flows. These predictions vary slightly depending on whether the larvae are strong or weak swimmers with respect to the ambient vertical velocities. Deshenieks et al. (1996) have modeled the vertical distribution of oyster larvae with respect to multiple environmental factors. Strong evidence that bivalve larval behavior matters comes chiefly from many demonstrations (studies cited above) that larvae of different species have different vertical distributions with respect to convergent and divergent flows, even though their size, shape, and mass may be very similar. One factor complicating this conclusion might occur when larvae are spawned into different water masses and maintain their fidelity to that water mass throughout most of their larval lives (e.g., Shanks et al. 2002, 2003a; Ma and Grassle 2004).

In the present study, we followed up on previous studies of near-bottom meroplankton abundances during upwelling and downwelling in the coastal environment at LEO-15 (Ma and Grassle 2004; Ma 2005) with a study of vertical larval distributions along a cross-shore transect during both upwelling and downwelling. The following hypotheses were examined: (1) during upwelling, larvae of all bivalve taxa are concentrated near the thermocline at an offshore divergent front; (2) during downwelling, larvae are concentrated where the downwelling front intersects the bottom inshore. Since surfclam larvae were expected to be the most abundant meroplanktonic species in July, when the study was done, we specifically predicted that they would have different distributions near shore during upwelling and downwelling, and that they would be concentrated above the thermocline in a stratified water column and more evenly distributed with respect to depth in a well-mixed water column. To examine whether ontogenetic changes in larval swimming behavior might contribute to different distributions in “young” larvae versus those

close to metamorphosis, we also measured shell lengths of larvae when concentrations were relatively high.

Materials and methods

On six dates in July 1998, mobile plankton pump samples were taken from five to six stations along transect A at LEO-15 (Fig. 1 and Table 1) where frequent ADCP and CTD measurements were carried out as part of comprehensive physical oceanographic studies (Glenn et al. 1998). The mobile zooplankton pump consists of (1) a sample intake on a metal frame, (2) an eductor floating at the sea surface, (3) a shipboard gasoline or electrical pump, (4) a plankton sample collecting unit having a 102- μm net and a barrel on board (Snelgrove et al. 1999). The flow rate was calibrated for each deployment at a station. The intake was covered by a 1-mm mesh to prevent large zooplankton, especially ctenophores, from blocking the intake and hoses. The intake was about 1 m below the surface when surface samples were taken. The intake was 1 m above the bottom (mab) for bottom samples. The position of the intake for samples near the thermocline was based on temperature profiles, monitored on a laptop on the boat connected by a cable to a CTD on the pump frame. The temperature and salinity sensors were near the intake for plankton samples. The plankton samples were preserved in 70% ethanol on board, and stained with Rose Bengal in the laboratory. The samples were sorted under a dissecting microscope. Identification of bivalve larvae depended on scanning electron micrographs from the laboratory of R. Lutz (also see Lutz 1985; Fuller and

Lutz 1989) and identification keys of Loosanoff et al. (1966) and Chanley and Andrews (1971). A recent genetic study (Hare and Weinberg 2005) has suggested that a subspecies of *Spisula solidissima* Dillwyn, *S. solidissima similis* Say which is generally regarded as a more southern, shallow subtidal species, occurs in Waquoit Bay, Massachusetts. There is no evidence that *S. s. similis* occurs in the LEO-15 area or anywhere along the coast of New Jersey. If it does, its larvae would not have been distinguished in the present study.

Adaptive sampling depended on sea surface temperature features from observed AVHRR imagery and sea surface currents using sea surface radar (OSCR) (S. Glenn, personal communication) early on the sampling day. On 9 July, 16 July, 24 July, and 27 July in 1998, a CTD (Sea Bird Seacast 19) was mounted on the mobile pump frame near the intake. On 9 July and 16 July, adaptive mobile sampling was carried out at five stations (Sta. A1, A1a [Node A], A2, A3, and A3a) (Table 1). Samples of 250 l (with three replicates) from the surface, thermocline, and bottom were taken when three layers could be well defined. On 16 July, more samples were collected near the thermocline (above, in, and below the thermocline). On 24 July and 27 July, mobile zooplankton pump samples were also taken at Sta. A4 and A5 (and Sta. A5a on 24 July). On two cruises (6 July and 14 July), the mobile plankton pump samples were taken without a CTD on the pump frame but temperature measurements from a sensor on a hand-lowered fluorometer were used to guide the plankton sampling. On the first trial cruise on 6 July, three replicate 250-l plankton samples from the surface and bottom were taken at six stations. On 14 July, plankton

Fig. 1 Bathymetric map of the LEO-15 research area and location of transect A and sampling stations (filled black circles) off Tuckerton, New Jersey, USA. Sta. A1a was near underwater node A where physical data were recorded (courtesy of Rutgers Marine Remote Sensing Laboratory)

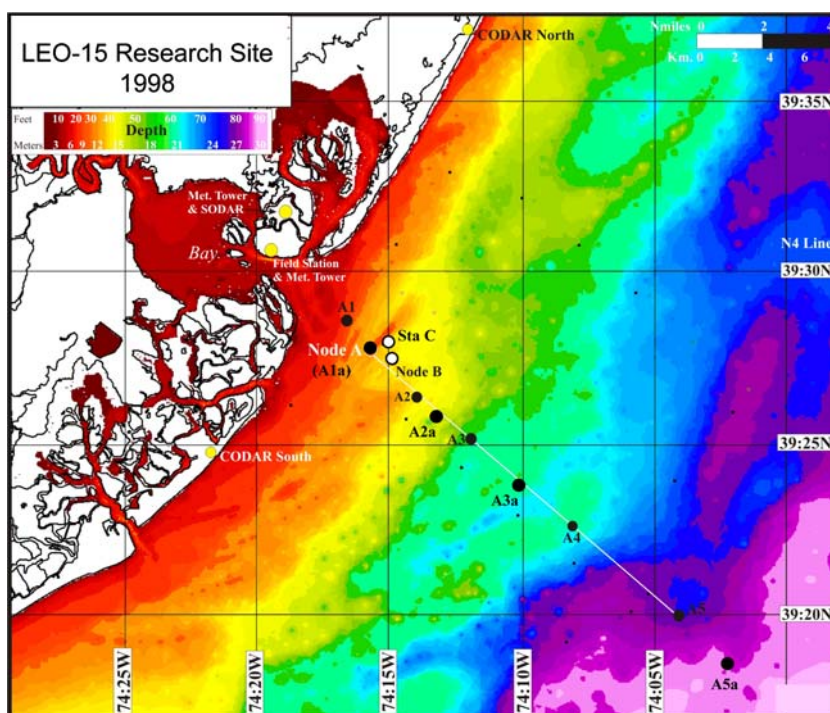


Table 1 Mobile zooplankton pump sampling along LEO-15 transect A in July 1998

Dates	Stations	Sampling depths	T measurements
6 July	A1, A1a, A2, A2a, A3, A3a	Surface and bottom	Fluorometer
9 July	A1, A1a, A2, A3, A3a	Surface, bottom, and thermocline	CTD
14 July	A1, A1a, A2, A2a, A3, A3a	Surface, bottom, and thermocline	Fluorometer
16 July	A1, A1a, A2, A3, A3a	1–3 Depths near thermocline	CTD
24 July	A1a, A2, A3, A4, A5, A5a	Surface, bottom, and thermocline	CTD
27 July	A1a, A2, A3, A4, A5	Surface, bottom, and thermocline	CTD

samples from the surface, thermocline, and bottom were taken at the same six stations. Except for 16 July (with samples from >three depths), the mid-depth samples were taken immediately above the 16°C isotherm. We were mostly interested in larval concentrations above the thermocline for mid-depth samples (see the hypotheses). The somewhat variable sampling regimes on different dates were adapted to prevailing conditions on each date and to logistic constraints (Table 1).

Wind and temperature data were analyzed and correlated with larval bivalve distributions. Wind data were from the Rutgers Marine Field Station meteorological tower (recorded every min). Time-series data for bottom temperature at an inshore station (Sta. C) were from the temperature sensor (every 4 h) on a Moored, Automated, Serial Zooplankton Pump (MASZP) moored 1 mab. A thermistor was also attached to the MASZP to record temperature every 12 min.

Larval surfclam and other larval bivalve concentrations were acquired at Sta. A1a, Sta. A2, and Sta. A3 on all sampling dates. Larval surfclam concentrations at Sta. A1a and Sta. A2 were analyzed by a two-way ANOVA with date and depth as fixed factors. The raw data for larval concentrations were log transformed to remove heterogeneity in variance. Larval surfclam concentrations were low (zero at some depths) at Sta. A3, and no transformations could achieve homogeneity of variances. An F_{\max} test (Sokal and Rohlf 1981) was used to examine homogeneity, and a qqnorm plot (Mathsoft 1998) for normality. Multiple comparisons were carried out using a Tukey test. Shell lengths of different taxa of bivalve larvae were measured with an ocular micrometer when larval concentrations were high enough (>100 ind. 250 l^{-1}). In some cases, shell length distributions were compared using a two-sample Wilcoxon test (non-parametric).

Results

Physical conditions

Adaptive mobile pump sampling was initiated on 6 July 1998. The winds from 5 July to 12 July were downwelling favorable (from NE) most of the time except for brief upwelling winds from 9–10 July (Fig. 2). Upwelling favorable winds (from SW) were dominant from 12 July to 25 July until downwelling winds occurred on 25 July

and 26 July. At an inshore station near LEO-15 node A, low bottom temperature persisted from 14 July to 25 July during upwelling.

On four sampling dates (9 July, 16 July, 24 July, and 27 July) when a CTD was attached to the mobile plankton pump, spatial temperature and salinity data were acquired. On 9 July and 16 July, adaptive mobile sampling was carried out at Sta. A1 (1.9 km offshore), A1a (3.5 km offshore, near LEO-15 Node A), A2 (6.7 km offshore), A3 (10.2 km offshore), and A3a (13.7 km offshore). On 9 July during downwelling, the thermocline was at ~ 10 m depth near shore and water temperature was uniform from surface to bottom ($>21^\circ\text{C}$) at Sta. A1 (~ 7 m deep) (Fig. 3). On 16 July during upwelling, the thermocline near shore was at ~ 5 m depth and water was stratified at Sta. A1. Surface temperature increased by 2°C from Sta. A1 to Sta. A1a, an indication of a surface front between these two stations. On 24 July and 27 July, samples were taken at Sta. A1a, A2, A3, A4 (17.2 km offshore), A5 (24.2 km offshore), and A5a (27.7 km offshore). On 24 July during upwelling, the thermocline was at ~ 7 m depth near shore and water was stratified near shore at Sta. A1a. Surface temperature gradients of a few degrees occurred between Sta. A1a and A2, and between Sta. A5 and A5a, indicating that surface fronts were present both near shore and further offshore. On 27 July during down-

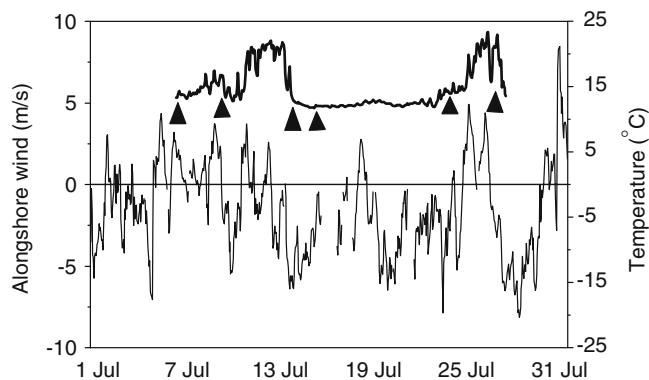
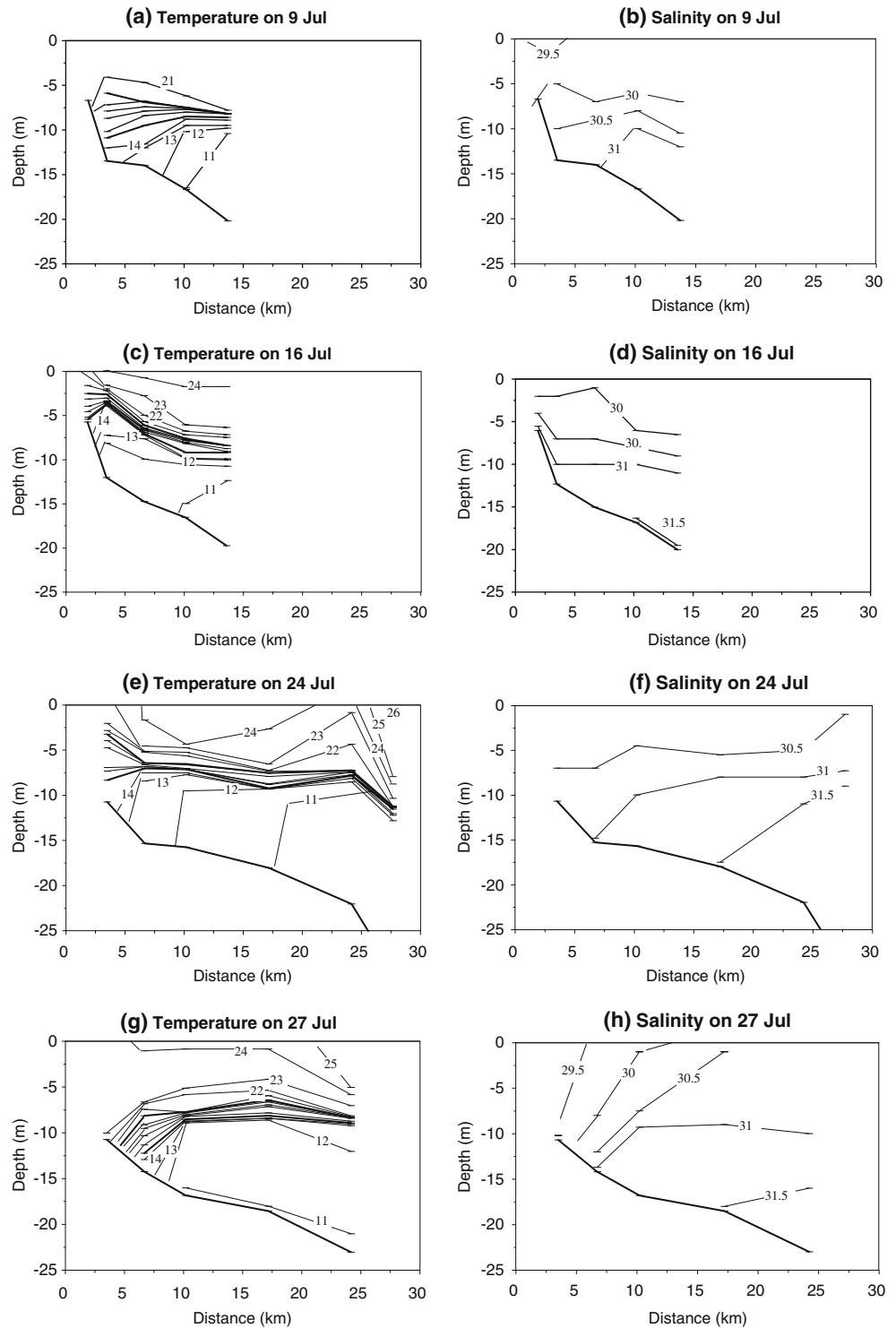


Fig. 2 Hourly averaged wind intensity (*thin line*) in alongshore direction (southwest or northeast) on 1 July to 31 July 1998. Winds with positive values were downwelling favorable (from NE). Hourly averaged bottom temperature (from a thermistor 1 mab) at an inshore station (1 km offshore from Node A) from 7 July to 27 July is shown with a *thick line*. Arrows indicate dates when mobile pump plankton samples were taken (6, 9, 14, 16, 24, and 27 July)

Fig. 3 Temperature and salinity profiles (from CTD measurements) on 9 July, 16 July, 24 July, and 27 July. The isotherms between *lower and upper thick lines* are 15, 16, 17, 18, 19, and 20°C. *Bottom thick line* is the bottom profile. *X axis* indicates distance of each station from the coast



welling, the thermocline was tilted down near shore and the water column was well mixed at Sta. A1a near shore.

On 16 July during upwelling, water with a salinity of 31 reached the bottom at Sta. A1. The salinity difference between surface and bottom water was > 1 (the difference was < 0.5 at Sta. A1 on 9 July during downwelling) (Fig. 3). On 27 July during downwelling, water of < 29.5 occurred at Sta. A1a, while salinity was > 30 at all sta-

tions on 24 July during upwelling. A cross-shelf salinity gradient was present near the surface on 27 July.

Larval surfclam distribution

The mean concentration of surfclam larvae on the transects ranged from 45.0 ind. 250 l⁻¹ on 9 July to 4.1

Table 2 Mean concentrations (SD) of larval surfclams (*S. solidissima*), *A. simplex*, pholads, *D. fossor*, and mytilids (ind. 250 l⁻¹)

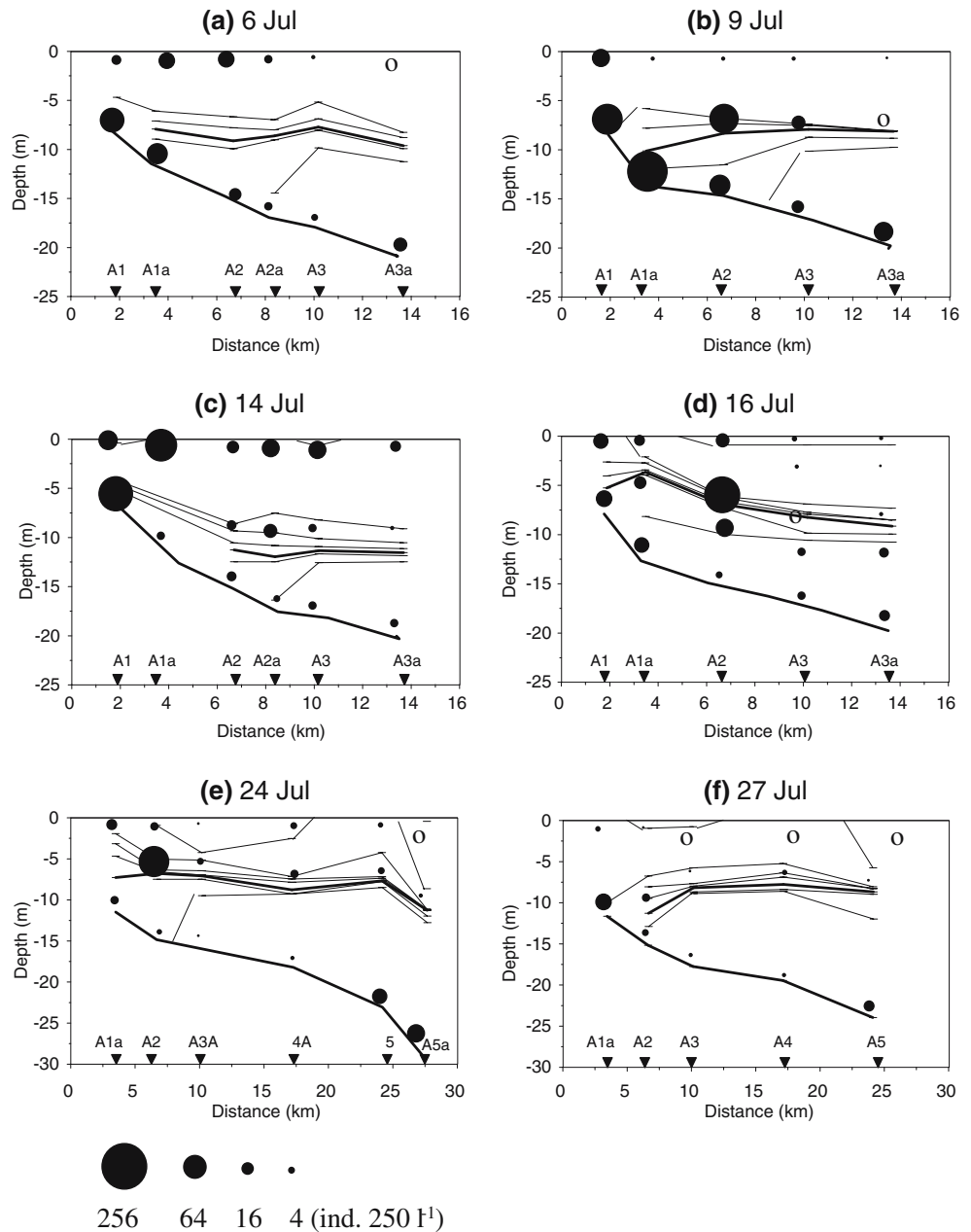
Dates	<i>S. solidissima</i>	<i>A. simplex</i>	Pholadidae	<i>D. fossor</i>	Mytilidae
6 July	20.9 (21.5)	5.0 (7)	3.4 (6.3)	0.1 (0.2)	26.6 (32.1)
9 July	45.0 (60.6)	5.8 (11.6)	4.6 (7.1)	2.9 (6.8)	34.6 (69.2)
14 July	29.7 (42.0)	1.5 (2.5)	12.7 (20.2)	14.8 (21.5)	38.0 (62.5)
16 July	20.6 (42.2)	8.2 (16.5)	1.2 (1.9)	10.0 (27.8)	27.0(42.1)
24 July	12.7 (25.7)	3.0 (6.5)	1.7 (4.1)	2.1 (3.7)	2.2 (3.2)
27 July	4.1 (8)	4.8 (11.6)	1.6 (4.8)	1.6 (3.1)	1.4 (2.6)

ind. 250 l⁻¹ on 27 July (Table 2). On 6 July, plankton samples were only taken from near the surface and near the bottom. The highest larval surfclam concentration (>3 times the mean) occurred at Sta. A1 at the bottom

(Fig. 4a). Larval surfclam concentration at Sta. A1a at the bottom was >2 times the mean.

On 9 July during downwelling, the highest concentration (>3 times the mean, and same definition for

Fig. 4 *S. solidissima*. Spatial distributions of surfclam larvae on 6 July, 9 July, 14 July, 16 July, 24 July, and 27 July 1998. Area of each solid circle is proportional to larval concentration at each location (open circles = no larvae). Thin lines are isotherms and temperature difference is 2°C between two adjacent isotherms (temperature is higher near surface). 16°C isotherm (thick line) is used as a proxy for the position of the thermocline. On 14 July, there were no temperature data for Sta. A1a. Bottom thick line represents bottom profile. Sampling stations are marked with triangles



highest concentration or most abundant hereafter) of surfclam larvae occurred near the bottom at Sta. A1a and high concentrations (>2 times the mean) of surfclam larvae were present at Sta. A1 near the bottom and at Sta. A2 near the thermocline (Fig. 4b). An upwelling started on 14 July. The highest larval surfclam concentrations occurred at Sta. A1 near the bottom and at Sta. A1a near the surface (Fig. 4c). On 16 July and 24 July during upwelling, surfclam larvae were most abundant at Sta. A2 above the thermocline. Larval surfclam concentration at Sta. A5a near the bottom was >2 times the mean on 24 July (Fig. 4d, e). On 27 July during downwelling, the highest concentration of surfclam larvae was at Sta. A1a near the bottom (Fig. 4f), and there were some surfclam larvae at Sta. A5 near the bottom (>2 times the mean).

The ANOVA tables show that date, depth, and the interaction between date and depth had significant effects on larval surfclam concentrations at Sta. A1a and A2 (Table 3). At Sta. A1a, larval surfclam concentrations were significantly higher near the bottom on 9 July and 27 July during downwelling, and the concentration was higher near the surface on 14 July when an upwelling had just started (Fig. 5a). At Sta. A2, the larval surfclam concentrations were significantly higher above (and near) the thermocline on 16 July and 24 July during upwelling (Fig. 5b). Overall, larval surfclam concentrations were much lower at Sta. A3 (Fig. 5c). In general, surfclam larvae were most abundant near the bottom at Sta. A1a during downwelling, and most abundant above the thermocline at Sta. A2 during upwelling.

The median shell length of surfclam larvae was similar between surface and bottom samples at Sta. A1 on 9 July during downwelling (Fig. 6). The median of larval shell length was larger near the bottom at Sta. A1a and A2. The surfclam larvae near the thermocline at Sta. A2 had intermediate shell lengths. On 14 July (upwelling), the shell length was smaller in larvae near the surface than near the bottom at Sta. A1 (Fig. 6), and at Sta. A1a (surface) the median larval length was only 187 μm . The

median shell lengths of surfclam larvae near the thermocline at Sta. A2 were 222 μm on 16 July (upwelling) and 257 μm on 24 July (upwelling). The median of surfclam larval shell length inshore (A1) was significantly larger near the bottom than near the surface (Wilcoxon rank-sum test, $z=7.477$, $P<0.0001$) when the temperature difference between surface and bottom waters was $>8^\circ\text{C}$ during upwelling (14 July). The medians were similar between surface and bottom samples inshore when the water was mixed during downwelling (9 July).

Larval distributions of other common bivalves

Other common bivalve larvae identified in the mobile pump plankton samples include *Anomia simplex*, *Donax fossor*, *Ensis directus*, *Mya arenaria*, Mytilidae spp. (called mytilid hereafter), Pholadidae spp. (pholad

Table 3 *S. solidissima*. ANOVA for larval surfclam concentrations (ind. 250 l^{-1}) at Sta. A1a, Sta. A2, and Sta. A3. Dates (9 July, 14 July, 16 July, 24 July, and 27 July 1998) and depths (surface and bottom for Sta. A1a, three depths for Sta. A2 and A3) were fixed factors

Sources	df	Sum of squares	Mean square	F value	P value
Sta. A1a					
Date	4	1.012	0.253	8.96	0.0003
Depth	1	0.926	0.926	32.83	0.0001
Date \times depth	4	9.792	2.448	86.76	0.0001
Error	20	0.564	0.028		
Sta. A2					
Date	4	5.407	1.352	20.14	0.0001
Depth	2	6.476	3.238	48.25	0.0001
Date \times depth	8	7.034	0.879	13.10	0.0001
Error	30	2.013	0.067		

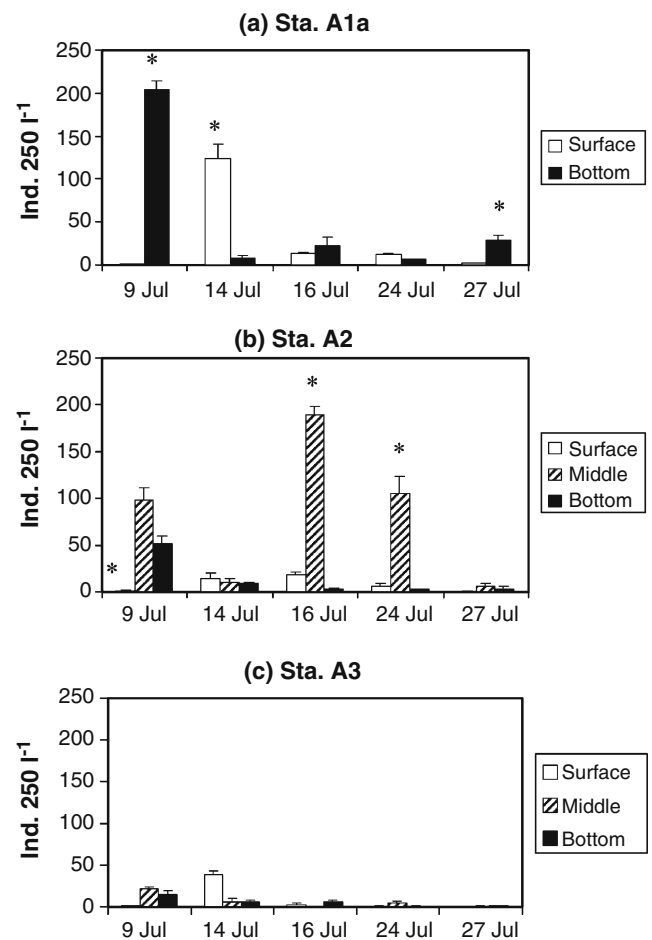


Fig. 5 *S. solidissima*. Mean larval surfclam concentrations (\pm SE) at Sta. A1a, A2, and A3. Star symbol indicates that larval concentration at one depth is significantly different from other depths at a station on a specific date based on Tukey tests. The values for Tukey tests were derived from mean square of error in Table 3. All the means within each station (Sta. A1a and Sta. A2) were compared simultaneously to have an overall type I error of 0.05

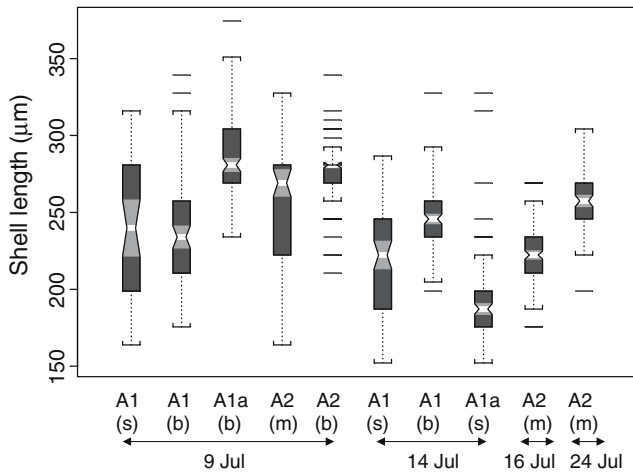


Fig. 6 *S. solidissima*. Boxplots for shell lengths of surfclam larvae in samples with high concentrations on 9 July (Sta. A1 [surface (s) and bottom (b)], Sta. A1a [bottom], Sta. A2 [middle (m) and bottom]), 14 July (Sta. A1 [surface and bottom], Sta. A1a [surface]), 16 July (Sta. A2 [above thermocline (m)]), and 24 July (Sta. A2 [middle]). *Open bars* in middle of boxes are medians. Upper and lower ends of boxes represent upper and lower fourths. *Brackets* linked to boxes by *dashed lines* are upper and lower outlier cut-offs. If notches on two boxes do not overlap, this indicates a significant difference in the medians ($\alpha=0.05$, Mathsoft 1998)

hereafter), *Tellina* spp., and *Teredo navalis*. We only present data for the bivalve species (taxa) that were most abundant and had the highest frequency of occurrence (Table 2).

The spatial distributions of *A. simplex* and pholad larvae were similar to those of surfclam larvae. On 6 July, the highest concentration of *A. simplex* larvae occurred at Sta. A2a near the bottom (Fig. 7). On 9 July during downwelling, the highest concentrations of *A. simplex* larvae were at Sta. A3 and A2 near the bottom. Few *A. simplex* larvae were present on 14 July (upwelling). Larval concentrations at Sta. A1 and A3 near the bottom were >3 times the mean. On 16 July during upwelling, *A. simplex* larvae were most abundant at Sta. A2 and near the thermocline at Sta. A1a. On 24 July (upwelling), the larvae were most abundant at Sta. A2 near the thermocline, and on 27 July (downwelling) most abundant at Sta. A2 near the bottom.

The highest concentrations of pholad larvae on 6 July were at Sta. A1 and A1a near the bottom (Fig. 8). On 9 July (upwelling), the highest concentration of pholad larvae occurred at Sta. A1a near the bottom. High larval concentrations (>2 times the mean) were also present at Sta. A2 near the bottom and near the thermocline. On 14 July (upwelling), pholad larvae were most abundant at Sta. A1 near the bottom and at Sta. A2a and A3 near the thermocline. Larval concentration on 16 July was ten times less than on 14 July. The highest concentration (at Sta. A1 near the bottom) was <10 ind. 250 l^{-1} . On 24 July (upwelling), the highest larval concentration was at Sta. A2 near the thermocline. On 27 July (downwelling), the highest larval concentration was at Sta. A1a near the

bottom. Overall, pholad larval distributions resembled those of surfclams and *A. simplex*.

There were very few *D. fossor* larvae present on 6 July (Fig. 9). On 9 July during downwelling, the highest larval *D. fossor* concentrations were present at Sta. A2 and A3 near the thermocline. On 14 July (upwelling), the larvae were most abundant at Sta. A1a and A2a near the surface and at Sta. A1 near the bottom. The highest larval concentrations on 16 July (upwelling) were at Sta. A1a and A2 near the surface. On 24 July (upwelling) the highest larval *D. fossor* concentration was at Sta. A1a near the surface, and on 27 July (downwelling) the highest concentrations were at Sta. A4 near the surface and near the thermocline. Most *D. fossor* larvae were found near the surface or near the thermocline.

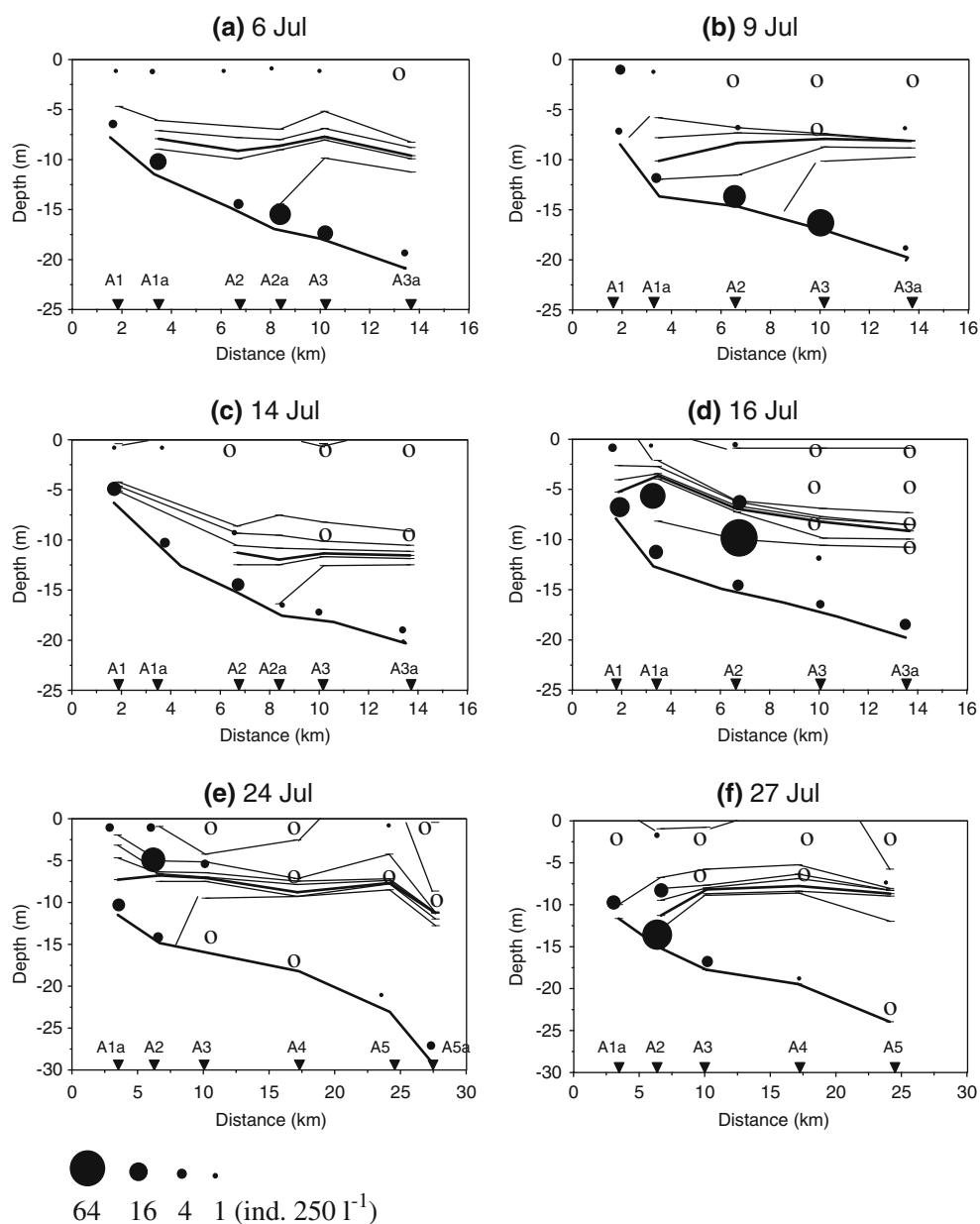
The concentrations of mytilid larvae on 6 July were >3 times the mean at Sta. A1a and A3 near the bottom (Fig. 10). On 9 July (downwelling), mytilid larvae were most abundant at Sta. A2 near the bottom. Larvae were also present in high numbers (>2 times the mean) at Sta. A3 near the bottom. On 14 July (upwelling), the highest concentrations were at Sta. A1 and A2 near the bottom. On 16 July (upwelling), the highest larval concentration was near the bottom at Sta. A2. High larval concentrations (>2 times the mean) also occurred at Sta. A1 near the bottom and at Sta. A1a near the bottom and near the thermocline. Larval concentrations were ten times lower on 24 July (upwelling) and 27 July (downwelling), when there were some larvae at Sta. A2 and A3 near the bottom. On all dates, very few mytilid larvae were present above the thermocline or near the surface.

The present study indicated that bivalve larvae had patchy distributions and that the distributions differed among taxa (Fig. 11). Dense patches were on a scale of several kilometers in a cross-shelf direction, and the patch locations differed between upwelling and downwelling conditions.

Discussion

The locations for patches of highest larval concentrations of different bivalve taxa are summarized in Fig. 11. The highest surfclam concentration during well-developed upwelling (16 July and 24 July) was at Sta. A2 (~ 7 km offshore) where isotherms tilted upward. That was where a surface upwelling jet (in an alongshore direction) was located on 16 July (Fig. 12). Chant et al. (2004) suggest that the vertical shear ($f \frac{\partial v}{\partial z}$) across the tilting thermocline is in thermal wind balance (i.e., $f \frac{\partial v}{\partial z} \approx \frac{g}{\rho} \times \frac{\partial \rho}{\partial x}$). Here, f is the Coriolis parameter, v , the alongshore velocity, and, ρ , the water density (x and z are in cross-shelf and vertical directions, respectively). However, above the thermocline where the alongshore jet resides, baroclinic forcing ($\frac{g}{\rho} \times \frac{\partial \rho}{\partial x}$) is weak. We suggest that the cross-shore momentum balance would be between the Coriolis shear forcing and friction ($f \frac{\partial v}{\partial z} \approx \frac{\partial^2 \tau_x}{\partial z^2}$), where τ_x is the frictional stress in the cross-

Fig. 7 *A. simplex*. Spatial distributions of *A. simplex* larvae on six dates in July 1998

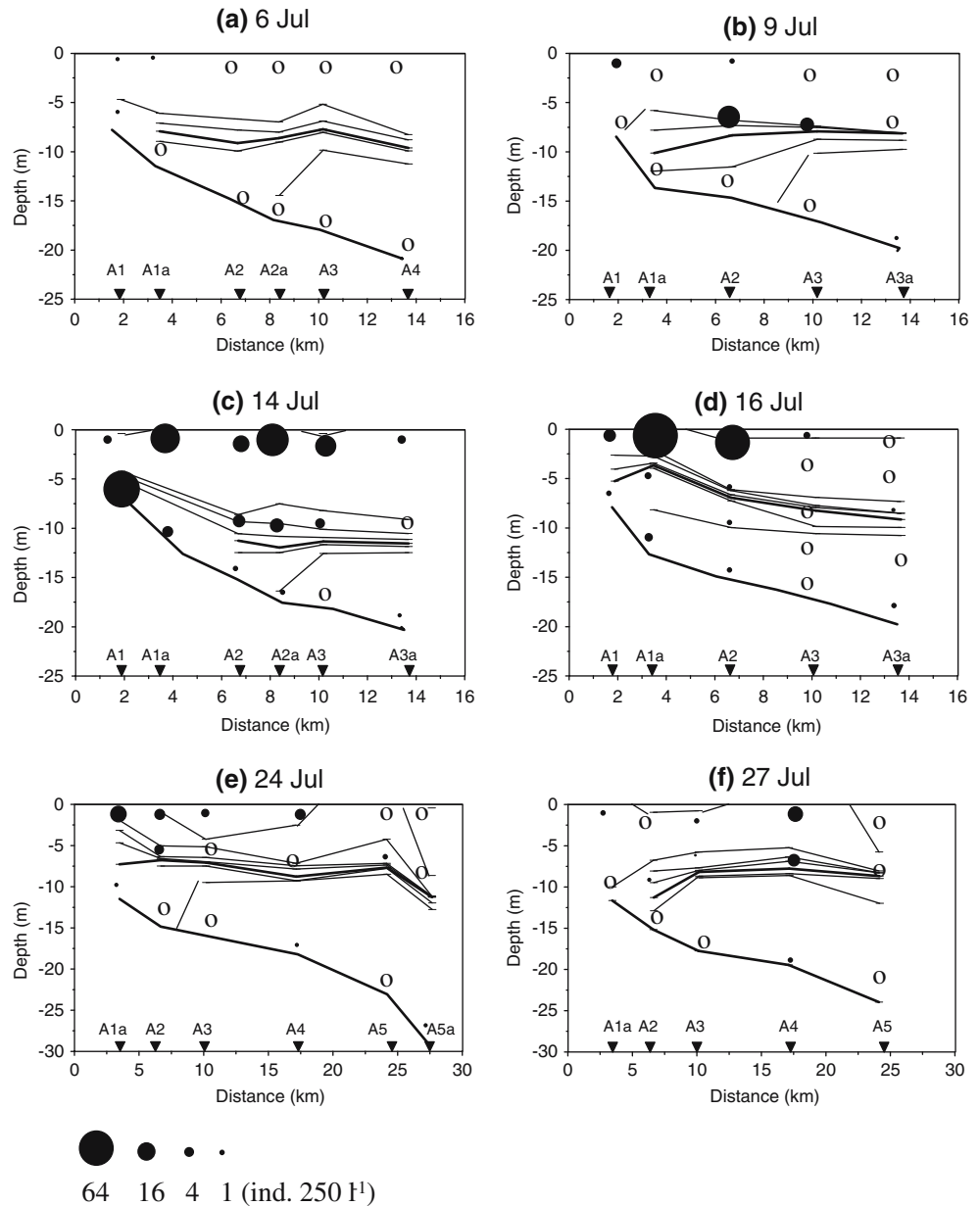


shelf direction. This balance has been assumed in theoretical models of coastal currents (e.g., Garrett et al. 1993) and can drive a clockwise secondary flow, with the upper part flowing offshore and the lower part of the jet onshore (Fig. 13). The superposition of this secondary flow with offshore Ekman flow can drive a convergence near the bottom of the jet and a divergence on the top. Such a convergence, combined with larval behavior (e.g., upward swimming and avoidance of descending below the thermocline) could concentrate surfclam larvae. The ADCP data from a transect 15 km north of transect A indicated that the upwelling jet (flowing to the north) on 24 July (i.e., when the upwelling was fully developed) was ~25 km from the coast (Chant et al. 2004). The high concentration of surfclam larvae occurring at Sta A2 on 24 July (7 km offshore) was near

the inshore side of a cyclonic eddy. On 14 July when the upwelling had only just begun to develop, a high larval concentration near the thermocline was not observed. Larvae were concentrated inshore (Sta. A1) and near the surface (Sta. A1a).

During downwelling, surfclam larvae were concentrated near the bottom at an inshore station (Sta. A1a) where water depths were similar to the position of the thermocline. It is likely that the larvae concentrated near the thermocline during upwelling were moved inshore along the thermocline and were brought to the sea floor when the thermocline intersected the bottom (Figs. 11, 13). It is also possible that the surfclam larvae only became concentrated as the downwelling front moved inshore, as suggested by Pineda (1999) and Shanks et al. (2000). Genin et al. (2005) suggested that swimming

Fig. 9 *D. fossor*. Spatial distributions of *D. fossor* larvae on six dates in July 1998



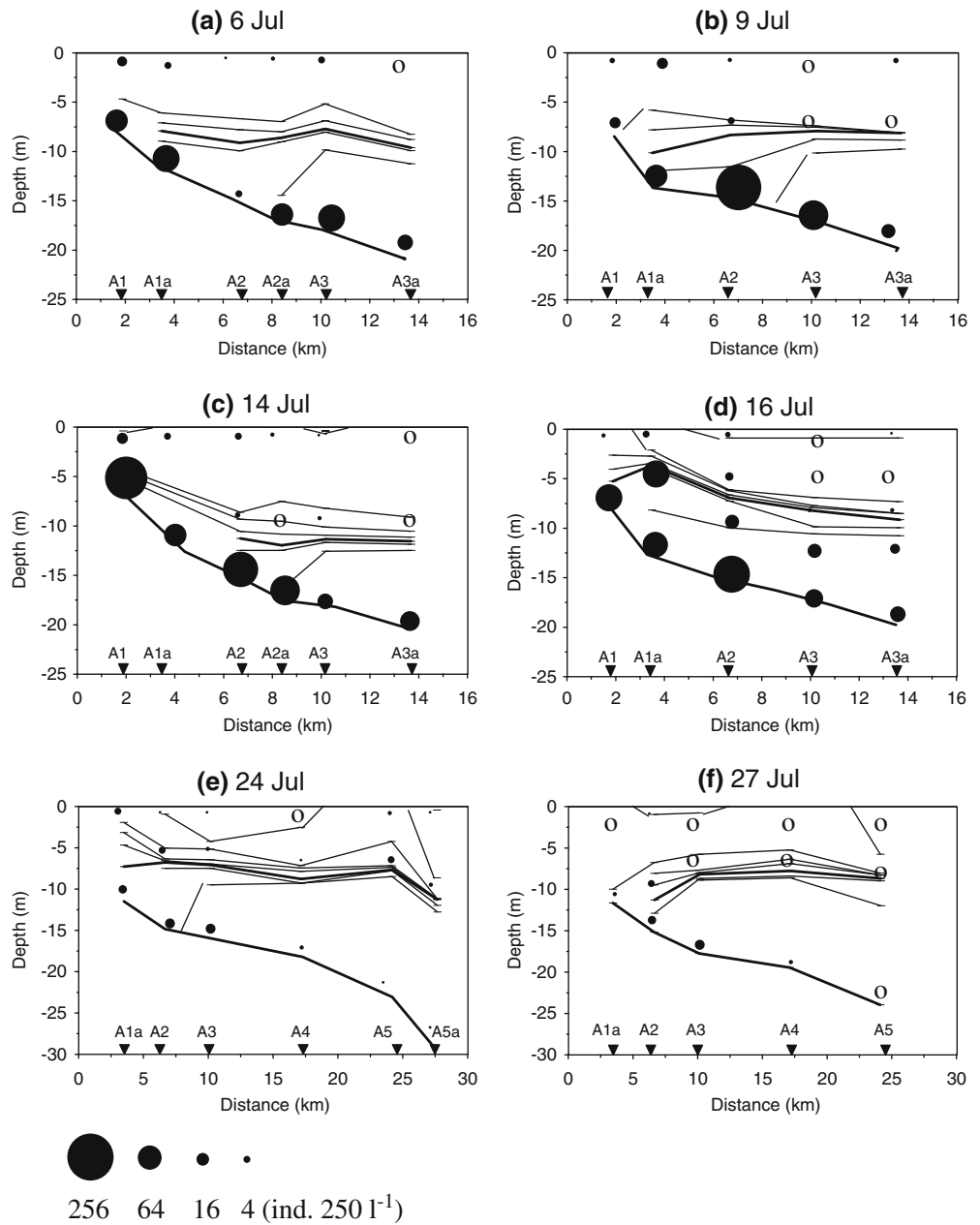
grated to the south on 23 July (Chant et al. 2004). Images of sea surface currents on both dates revealed a strong nearshore southerly flow of cool water that turned offshore over the rougher topography at the inshore side near transect A (Chant et al. 2004). We observed many scyphomedusae at the surface at Sta. A5, but no concentration of bivalve larvae related to this offshore strong surface temperature gradient was observed in the plankton samples. The high concentration of surfclam larvae inshore during coastal upwelling at Sta A2 on 24 July was near the inshore surface front. This may suggest that surfclam larvae are not passively carried offshore to a great distance during upwelling.

The shell lengths of surfclam larvae were measured in samples from several locations on 9 July (downwelling) and 14 July (upwelling). The surfclam larvae below the

thermocline, when the water column was strongly stratified, were mostly $> 250 \mu\text{m}$, similar to shell lengths of competent surfclam larvae in laboratory studies (Snelgrove et al. 1998). In a previous study at LEO-15 in August–September 1994, surfclam larvae near the bottom were larger than those near the surface under stratified conditions during upwelling (Ma 1997), consistent with the findings from the present study.

As a comparison, mesocosm studies have shown that sea scallop (*Placopecten magellanicus*) larvae seldom occurred below the thermocline until they reached a shell length of $\sim 200 \mu\text{m}$ (Gallager et al. 1996; Manuel et al. 2000), approaching the 230–260 μm shell length at metamorphosis (Culliney 1974). The vertical swimming behavior of surfclam larvae may similarly keep them above the thermocline until they reach a certain size. The

Fig. 10 *F. Mytilidae*. Spatial distributions of mytilid larvae on six dates in July 1998



similarity in larval size between surface and bottom samples at Sta. A1 on 9 July may be due to the lack of temperature stratification and/or vigorous mixing in a shallow water column (~7 m deep).

Shanks et al. (2002, 2003a), in the studies off Duck, North Carolina in mid- to late August 1994, concluded that surfclam larvae belonged to a group of taxa whose larvae were behaving as passive particles and were found in highest concentrations below the pycnocline during both upwelling and downwelling. In Shanks' studies, the larvae were concentrated in waters below the thermocline with temperatures of 18–20°C, temperatures that are similar to the temperatures in the waters above and near the thermocline where high concentrations of

surfclams were found in the present study. It is probable that the surfclam larvae at the more southern site (Duck, North Carolina) in August (Shanks et al. 2002, 2003a) were produced by spawning of clams living below the thermocline (bottom temperatures were >16°C below the thermocline). We believe that surfclams collected in July at LEO-15 were from spawning of surfclams in inshore waters as they warmed in May and June (see Ma and Grassle 2004 for discussion). In both studies, surfclam larvae were moved back and forth with upwelling and downwelling, and they appeared to stay with the water mass in which they were spawned, at least until they reached a shell length when they were close to settlement and metamorphosis.

Fig. 11 Presentation of larval patches for **a** *S. solidissima*, **b** *A. simplex*, **c** pholads, **d** *D. fossor*, and **e** mytilids. Patches are defined for locations with larval concentrations > (mean + 2 SD). Line tilted upward shows general position of thermocline during upwelling, and line tilted downward indicates thermocline during downwelling. U1, U2, U3 represent upwellings on 14 July, 16 July, and 24 July. D1 and D2 are downwellings on 9 July and 27 July

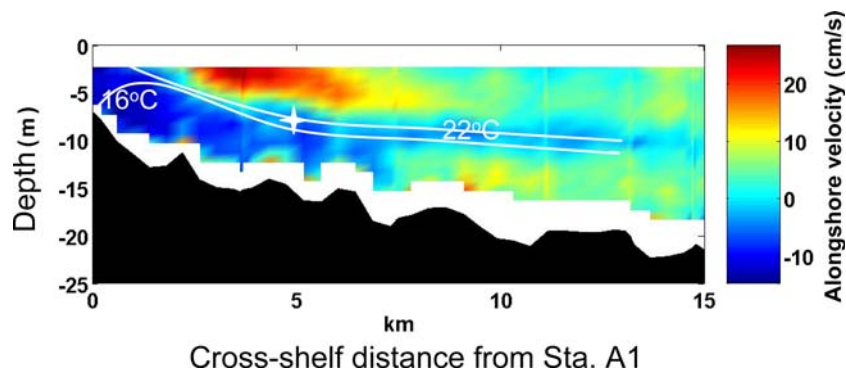
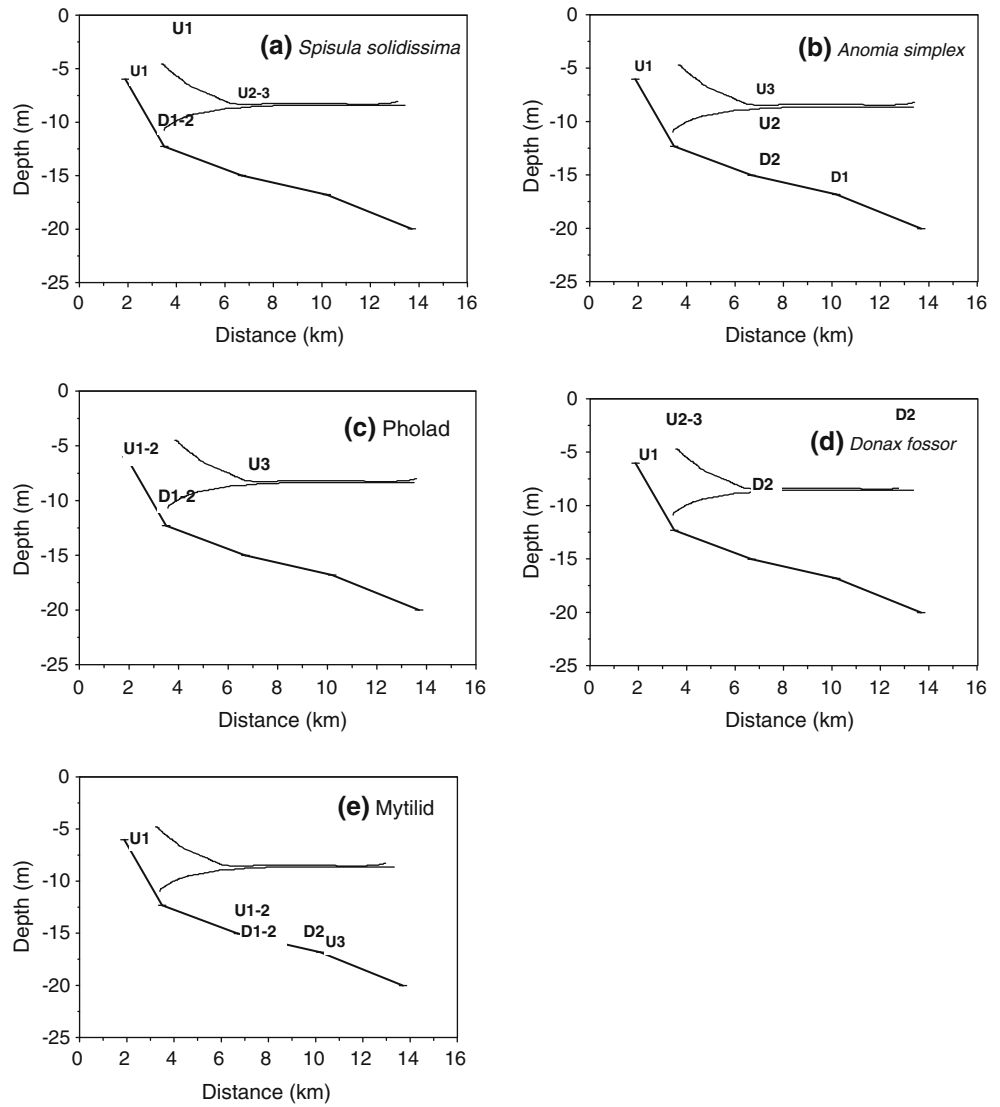


Fig. 12 Alongshore currents from ADCP tow on transect A, 16 July 1998. The measurements started from Sta. A1 inshore, and gaps near surface and near bottom were where ADCP could not make measurements. Positive values are toward north. *Star symbol*

indicates location of highest larval surfclam concentrations during upwelling. Note alongshore jet (above thermocline) inshore. 16 and 22°C isotherms are superimposed to show location of thermocline and stratification of water temperature

In general, the spatial distributions of *A. simplex* and pholad larvae were similar to those of surfclam larvae: larvae were found near the bottom during downwelling

and they were concentrated near the thermocline during upwelling. During downwelling, the patches of high larval *A. simplex* concentrations were near the bottom at

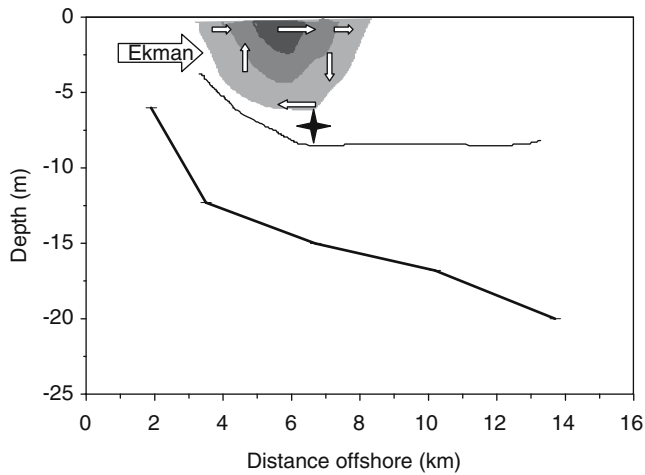


Fig. 13 Conceptual model of larval surfclam concentrating mechanism. Shaded regions indicate an upwelling jet flowing into the page. Open arrows represent the secondary flows, of different magnitudes. Solid line is thermocline during upwelling, Star symbol represents location of highest larval surfclam concentration

Sta. A2 and A3. At the initiation of the upwelling, the larvae were found inshore near the bottom, and they were advected into the water column and concentrated near the thermocline as the upwelling intensified. However, the highest concentration of *A. simplex* larvae during downwelling was found further offshore than for surfclam larvae. The concentration during upwelling on 16 July was below the thermocline (above the thermocline for surfclams). The sources of *A. simplex* larvae at LEO-15 are unknown, and may be different from larval surfclam sources, explaining the small differences in distribution. Differences in larval swimming (or sinking) behavior could also account for the differences. Shell lengths of *A. simplex* larvae on 16 July indicated that

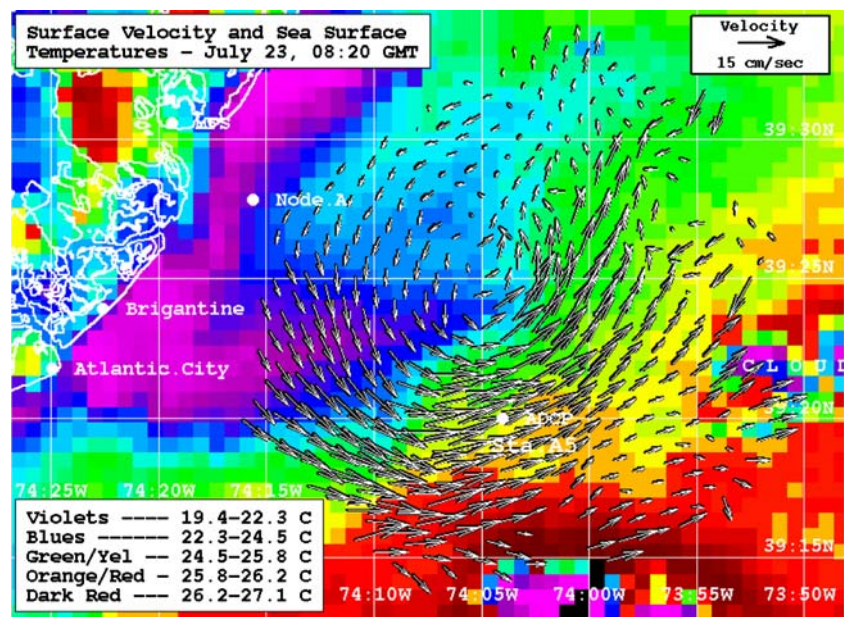
most of them were $>210 \mu\text{m}$. Shell length at metamorphosis is 195–210 μm in the laboratory (Loosanoff et al. 1966). This suggests that they could have been resuspended post-larvae or larvae delaying metamorphosis, and might have spent more time sinking (less actively swimming) than surfclam larvae.

Pholad larvae found in the mobile plankton samples were *Barnea truncata* or *Cyrtopleura costata*, or a combination of both. Like surfclam larvae, pholad larvae were concentrated near the bottom at Sta. A1a during downwelling, and when the upwelling was fully developed on 24 July high abundances were present above the thermocline at Sta. A2. On 14 July when the upwelling had just begun and on 16 July during upwelling, pholad larvae occurred in highest concentrations at Sta. A1 near the bottom. Adult pholad bathymetric distributions (*B. truncata* or *C. costata*) in this area are generally unknown. In a separate study, pholad larvae were found in samples collected in Barnegat Bay inlet (near LEO-15) in late June (Gregg 2002).

D. fossor and mytilid larvae had different distribution patterns from surfclams. *D. fossor* larvae were mostly found near the surface. This species does occur in benthic communities in the LEO-15 area (Garlo et al. 1979), but their life history is unknown. The *D. fossor* larvae in the present study were likely spawned in spring or early summer. The shell lengths for *D. fossor* larvae on 16 July were close to sizes of *D. variabilis* at metamorphosis [275–340 μm (Chanley 1969; Chanley and Andrews 1971)], but they were seldom found below the thermocline. If larvae of *D. fossor* and *D. variabilis* settle at similar sizes, it seems counterintuitive to find potentially competent *D. fossor* larvae occurring only above the thermocline.

Most of the mytilid larvae were found near the bottom. Their shell lengths (300–400 μm) indicated that most were ready to settle or were post-larvae. On 16 July

Fig. 14 Cyclonic eddy over transect A on 23 July 1998 with surface currents from sea surface radar and sea surface temperature from satellite imagery (courtesy of Rutgers Marine Remote Sensing Laboratory)



during upwelling, many mytilid larvae were also found in the middle of the water column at Sta. A1a, and shell lengths were similar to those of larvae in bottom samples. Most of these mytilid larvae were likely *Mytilus edulis*, based on features in the shell hinge of a subsample (Fuller and Lutz 1989). *M. edulis* is found from estuaries to depths of several hundred feet offshore (Gosner 1987). Its larvae metamorphose at shell lengths of 215–305 μm (Chanley and Andrews 1971). Martel et al. (2000) noted the marked contrast between the larval shell (prodissoconch II) and the juvenile (dissoconch) shell for postlarvae of *M. californianus* and *M. trossulus*. Similar marks were observed on the shells of some *M. edulis* individuals in our samples, suggesting that some were indeed postlarvae.

Except for the *D. fossor* larvae, which were found near the surface, all other bivalve larvae were present in highest concentrations near the thermocline at Sta. A1a (surfclam and pholad) or near the bottom further offshore (*A. simplex* and mytilid) during downwelling. On 14 July, larvae from all taxa had their highest concentration at Sta. A1 near the bottom, suggesting that all the bivalve larvae were initially transported inshore just as the upwelling was initiated. High concentrations of surfclam, pholad, and *D. fossor* larvae also occurred up in the water column at other stations on this date. During upwelling on 16 July and 24 July, surfclam larvae and *A. simplex* larvae (and pholads on 24 July) were concentrated near the thermocline at Sta. A2. On those same dates, however, the highest concentrations were near the surface for *D. fossor* and near the bottom for mytilids. The difference may be due to different larval behaviors such as swimming and sinking and/or different larval source populations (inshore vs. offshore). The interactions between larval behaviors and physical circulation, in addition to varying among species, may also change during larval development.

In summary, the present study revealed the inner shelf locations of high larval surfclam concentrations at LEO-15 during July upwelling and downwelling conditions. The highest larval density during upwelling was above the thermocline 7 km from shore where the thermocline tilted up sharply, and this concentration may result from a convergence produced by offshore Ekman transport and the vertical shear in an upwelling jet. During downwelling, high concentrations of surfclam larvae were near the bottom inshore where the water depth was similar to the thermocline depth. These patterns are consistent with the results from moored zooplankton pump samples in our previous study at two inshore stations near Sta. A1a (Ma and Grassle 2004). While the larvae of *A. simplex* and pholads showed similar patterns to surfclams, *D. fossor* and mytilid larvae had different distribution patterns. An integral knowledge of physical circulation, larval sources, and taxon-specific larval behavior will be needed to fully understand the impact of upwelling and downwelling on larval bivalve distributions and their settlement and recruitment.

Acknowledgements We thank Fred Grassle, Jeanine Rosario, Chris Gregg, Jennifer Gregg, Pam Nelson, and Jessica Vanisko for their help with the field sampling. Tara Hitchner, David Hutnick, and Alexander Soranno helped in sorting samples. Scott Glenn provided instantaneous physical information in July 1998. Trish Bergmann shared temperature data from the fluorometer measurements made by Oscar Schofield's laboratory. John Zlotnik, captain of Rutgers R/V "Arabella", provided assistance with field sampling. We thank Cheryl Ann Zimmer, Fred Grassle, and Gary Taghon for their comments on an early draft. Dr. Alan Shanks pointed out the difference in larval distribution patterns between our study and his and provided useful comments while reviewing another manuscript of ours. Comments from Dr. Roger Mann and an anonymous reviewer improved the manuscript. Mike Crowley, Josh Kohut, and Courtney Kohut helped with Fig. 1. This study was supported by a NOAA/NURP grant to Rutgers University.

References

- Baker P (2003) Two species of oyster larvae show different depth distributions in a shallow, well-mixed estuary. *J Shellfish Res* 22:733–736
- Baker P, Mann R (2003) Late stage bivalve larvae in a well-mixed estuary are not inert particles. *Estuaries* 26:837–845
- Chanley P (1969) Larval development of the coquina clam, *Donax variabilis* Say, with a discussion of the structure of the larval hinge in the Tellinacea. *Bull Mar Sci* 19:214–224
- Chanley P, Andrews JP (1971) Aids for identification of bivalve larvae of Virginia. *Malacologia* 11:45–119
- Chant RJ, Glenn SM, Kohut J (2004) Flow reversals during upwelling conditions on the New Jersey inner shelf. *J Geophys Res* 109:C12S03
- Connolly SR, Roughgarden J (1999) Increased recruitment of northeast Pacific barnacles during the 1997 El Niño. *Limnol Oceanogr* 44:466–469
- Culliney JL (1974) Larval development of the giant sea scallop *Placopecten magellanicus* (Gmelin). *Biol Bull* 147:321–332
- Desheniaks MM, Hofmann EE, Klinck JM, Powell EN (1996) Modeling the vertical distribution of oyster larvae in response to environmental conditions. *Mar Ecol Prog Ser* 136:97–110
- Farrell TM, Bracher D, Roughgarden J (1991) Cross-shelf transport causes recruitment to intertidal populations in central California. *Limnol Oceanogr* 36:219–288
- Franks PJS (1992) Sink or swim: accumulation of biomass at fronts. *Mar Ecol Prog Ser* 82:1–12
- Fuller SC, Lutz RA (1989) Shell morphology of larval and post-larval mytilids from the north-western Atlantic. *J Mar Biol Ass UK* 69:181–218
- Gallager SM, Manuel JL, Manning DA, O'Dor R (1996) Ontogenetic changes in the vertical distribution of giant scallop larvae, *Placopecten magellanicus*, in 9-m deep mesocosms as a function of light, food, and temperature stratification. *Mar Biol* 124:679–692
- Garland ED, Zimmer CA (2002) Hourly variations in planktonic larval concentrations on the inner shelf: emerging patterns and processes. *J Mar Res* 60:311–325
- Garland ED, Zimmer CA, Lentz SJ (2002) Larval distributions in inner-shelf waters: The roles of wind-driven cross-shelf currents and diel vertical migrations. *Limnol Oceanogr* 47:803–817
- Garlo EV, Milstein CB, Jahn AE (1979) Impact of hypoxic conditions in the vicinity of Little Egg Inlet, New Jersey in summer 1976. *Estuar Coast Mar Sci* 8:421–432
- Garrett C, MacCready P, Rhines P (1993) Boundary mixing and arrested Ekman layers: rotating stratified flow near a sloping boundary. *Ann Rev Fluid Mech* 25:291–323
- Genin A, Jaffe JS, Reef R, Richter C, Franks PJS (2005) Swimming against the flow: a mechanism of zooplankton aggregation. *Science* 308:860–862
- Glenn SM, Crowley MF, Haidvogel DB, Song YT (1996) Underwater observatory captures coastal upwelling events off New Jersey. *Eos, Trans, Am Geophys Union* 77:233–236

- Glenn SM, Haidvogel DB, Schofield OM, von Alt CJ, Levine ER (1998) Coastal predictive skill experiments. *Sea Technol*:63–69
- Gosner KL (1987) A field guide to the Atlantic seashore. The Peterson Field Guide Series. Houghton Mifflin Company, Houston
- Grassle JP, Snelgrove PVR, Butman CA (1992) Larval habitat choice in still water and flume flows by the opportunistic bivalve *Mulinia lateralis*. *Neth J Sea Res* 30:33–44
- Gregg CS (2002) Effects of biological and physical processes on the vertical distribution and horizontal transport of bivalve larvae in an estuarine inlet. PhD dissertation, Rutgers University
- Hare MP, Weinberg JR (2005) Phylogeography of surfclams, *Spisula solidissima*, in the western North Atlantic based on mitochondrial and nuclear DNA sequences. *Mar Biol* 146:707–716
- Kohut JT, Glenn SM, Chant RJ (2004) Seasonal current variability on the New Jersey inner shelf. *J Geophys Res* 109:C07S07
- Loosanoff VL, Davis HC, Chanley PE (1966) Dimensions and shapes of larvae of some bivalve mollusks. *Malacologia* 4:351–435
- Lutz RA (1985) Identification of bivalve larvae and postlarvae: a review of recent advances. *Am Malacological Bull Special Edition* 59–78
- Ma H (1997) Time series analyses of meroplankton in moored pump samples at LEO-15: The relationship between the abundance of surfclam larvae and nearshore upwelling events. MS thesis, Rutgers University
- Ma H (2005) Spatial and temporal variation in surfclam (*Spisula solidissima*) larval supply and settlement on the New Jersey inner shelf during summer upwelling and downwelling. *Estuar Coast Shelf Sci* 62:41–53
- Ma H, Grassle JP (2004) Invertebrate larval availability during summer upwelling and downwelling on the inner continental shelf off New Jersey. *J Mar Res* 62:837–865
- Ma H, Grassle JP, Rosario JM (2006). Initial recruitment and growth of surfclams (*Spisula solidissima* Dillwyn) on the inner continental shelf of New Jersey. *J Shellfish Res* (in revision)
- Mann R, Campos BM, Luckenbach MW (1991) Swimming rate and responses of larvae of three macrid bivalves to salinity discontinuities. *Mar Ecol Prog Ser* 68:257–269
- Manuel JL, Gallagher SM, Pearce CM, Manning DA, O'Dor RK (1996) Veligers from different populations of sea scallop *Placopecten magellanicus* have different vertical migration patterns. *Mar Ecol Prog Ser* 142:147–163
- Manuel JL, Pearce CM, Manning DA, O'Dor RK (2000) The response of sea scallop (*Placopecten magellanicus*) veligers to a weak thermocline in 9-m deep mesocosms. *Mar Biol* 137:169–175
- Martel AL, Auffrey LM, Robles CD, Honda BM (2000) Identification of settling and early postlarval stages of mussels (*Mytilus* spp.) from the Pacific coast of North America, using prodissoconch morphology and genomic DNA. *Mar Biol* 137:811–818
- MathSoft Inc (1998) S-Plus User's Guide. Version 4.5. MathSoft, Inc., Seattle, WA
- Miller BA, Emlet RB (1997) Influence of nearshore hydrodynamics on larval abundance and settlement of sea urchins *Strongylocentrotus franciscanus* and *S. purpuratus* in the Oregon upwelling zone. *Mar Ecol Prog Ser* 48:83–94
- Münchow A, Chant RJ (2000) Kinematics of inner shelf motions during the summer stratified season off New Jersey. *J Phys Oceanogr* 30:247–268
- Pearce CM, Gallagher SM, Manuel JL, Manning DA, O'Dor RK, Bourget E (1996) Settlement of larvae of the giant scallop, *Placopecten magellanicus*, in 9-m deep mesocosms as a function of temperature stratification, depth, food, and substratum. *Mar Biol* 124:693–706
- Pearce CM, Gallagher SM, Manuel JL, Manning DA, O'Dor RK, Bourget E (1998) Effect of thermoclines and turbulence on depth of larval settlement and spat recruitment of the giant scallop *Placopecten magellanicus* in 9.5 m deep laboratory mesocosms. *Mar Ecol Prog Ser* 165:195–215
- Pineda J (1999) Circulation and larval distribution in internal tidal bore warm fronts. *Limnol Oceanogr* 44:1400–1414
- Roughgarden J, Pennington JT, Stoner D, Alexander S, Miller K (1991) Collisions of upwelling fronts with the intertidal zone: the cause of recruitment pulses in barnacle populations of central California. *Acta Ecologica* 12:35–51
- Shanks AL, McCulloch A (2003) Topographically generated fronts, very nearshore oceanography, and the distribution of chlorophyll, detritus, and selected diatom and dinoflagellate taxa. *Mar Biol* 296:113–126
- Shanks AL, Largier J, Brink L, Brubaker J, Hooff R (2000) Demonstration of the onshore transport of larval invertebrates by the shoreward movement of an upwelling front. *Limnol Oceanogr* 45:230–236
- Shanks AL, Largier J, Brink L, Brubaker J, Hooff R (2002) Observations on the distribution of meroplankton during a downwelling event and associated intrusion of the Chesapeake Bay estuarine plume. *J Plankton Res* 24:391–416
- Shanks AL, Largier J, Brubaker J (2003a) Observations on the distribution of meroplankton during an upwelling event. *J Plankton Res* 25:645–667
- Shanks AL, McCulloch A, Miller J (2003b) Topographically generated fronts, very nearshore oceanography and the distribution of larval invertebrates and holoplankters. *J Plankton Res* 25:1251–1277
- Smith RL (1981) A comparison of the structure and variability of the flow field in three coastal upwelling regions: Oregon, Northeast Africa, and Peru. In: Richards FA (ed) Coastal upwelling. American Geophysical Union Washington, DC, pp 107–118
- Snelgrove PVR, Grassle JP, Butman CA (1998) Sediment choice by settling larvae of the bivalve, *Spisula solidissima* (Dillwyn), in flow and still water. *J Exp Mar Biol Ecol* 231:171–190
- Snelgrove PVR, Grassle JP, Grassle JF, Petrecca RF, Ma H (1999) In situ habitat selection by settling larvae of marine soft-sediment invertebrates. *Limnol Oceanogr* 44:1341–1347
- Snelgrove PVR, Grassle JF, Grassle JP, Petrecca RF, Stocks KI (2001) The role of colonization in establishing patterns of community composition and diversity in shallow-water sedimentary communities. *J Mar Res* 59:813–831
- Sokal RR, Rohlf FJ (1981) Biometry. 2nd edn. W. H. Freeman, New York
- Song YT, Haidvogel DB, Glenn SM (2001) Effects of topographic variability on the formation of upwelling centers off New Jersey: a theoretical model. *J Geophys Res* 106:9223–9240
- Tremblay MJ, Sinclair M (1990) Sea scallop larvae *Placopecten magellanicus* on Georges Bank: vertical distribution in relation to water column stratification and food. *Mar Ecol Prog Ser* 61:1–15
- Tremblay MJ, Loder JW, Werner FE, Naimie CE, Page FH, Sinclair MM (1994) Drift of sea scallop larvae *Placopecten magellanicus* on Georges Bank: a model study of the roles of mean advection, larval behavior and larval origin. *Deep-Sea Res II* 41:7–49
- Weissberger EJ, Grassle JP (2003) Settlement, first-year growth, and mortality of surfclams, *Spisula solidissima*. *Estuar Coast Shelf Sci* 56:669–684
- Wing SR, Largier JL, Louis WB, James FQ (1995a) Settlement and transport of benthic invertebrates in an intermittent upwelling region. *Limnol Oceanogr* 40:316–329
- Wing SR, Botsford LW, Largier JL, Morgan LE (1995b) Spatial structure of relaxation events and crab settlement in the northern California upwelling system. *Mar Ecol Prog Ser* 128:199–211
- Wing RS, Botsford LW, Ralston SV, Largier JL (1998) Meroplanktonic distribution and circulation in coastal retention zone of the northern California upwelling system. *Limnol Oceanogr* 43:1710–1721
- Yankovsky AE, Garvine RW, Münchow A (2000) Mesoscale currents on the inner New Jersey shelf driven by the interaction of buoyancy and wind forcing. *J Phys Oceanogr* 30:2214–2230